Electron–ion interactions for trapped highly charged Ge ions

G. Machtoub, J.R. Crespo López-Urrutia, X. Zhang, and H. Tawara

Abstract: A theoretical simulation of complex K X-ray spectra including those from dielectronic recombination and excitation processes is presented for trapped highly charged germanium ions (Ge^{q+}, $q = 27$–30) interacting with a dense electron beam. We carried out numerical calculations of transition rates, level energies, transition wavelengths, resonance and collision strengths, and satellite intensity factors. Analytical results related to cross sections of B- through He-like Ge ions were obtained as well. The simulated spectra, including the contribution from different charge states of Ge^{27+}–Ge^{30+}, show good overall agreement over a wide electron energy range with the available X-ray measurements from the Heidelberg electron beam ion trap (EBIT). We have also predicted the electron impact excitation cross-section ratios for different transitions of Ge^{29+} and Ge^{30+} ions. It should be emphasized that the present analysis can also provide new information and clues of possible temperature measurements for EBIT and other plasma diagnostics.

PACS No.: 32.30.Rj

Résumé : Nous présentons une simulation théorique du spectre X complexe, incluant les recombinaisons diélectroniques et les mécanismes d'excitation d'ions de Ge hautement chargés (Ge^{q+}, $q = 27$–30) en interaction avec un intense faisceau d'électrons. Nous avons complété des calculs de taux de transition, de niveaux d'énergie, de longueurs d'onde de transition, de forces de résonance/collision et des facteurs satellites d'intensité et obtenu des résultats analytiques pour des ions Ge de type B à He. Les spectres simulés, incluant la contribution des différents états de charge de Ge^{27+}–Ge^{30+}, montrent un bon accord sur un large domaine d'énergie des électrons avec les mesures X EBIT faites à Heiderberg. Nous avons aussi prédit la section efficace d'excitation d'impact électronique pour différentes transitions des ions Ge^{29+} et Ge^{30+}. Nous insistons sur le fait que la présente étude peut aussi fournir de nouveaux renseignements et indices sur de possibles mesures de température pour EBIT et d'autres diagnostiques du plasma.

[Traduit par la Rédaction]

Received 16 March 2005. Accepted 15 December 2005. Published on the NRC Research Press Web site at http://cjp.nrc.ca/ on 20 February 2006.

G. Machtoub.[1] Institute for Laser Science, Tokyo 182-8585, Japan.
J.R. Crespo López-Urrutia and H. Tawara. Max-Planck-Institut für Kernphysik, Saupfercheckweg 1, D-69117 Heidelberg, Germany.
X. Zhang. Applied Ion Beam Physics Laboratory, Institute of Modern Physics, Fudan University, Shanghai 200433, Republic of China.

[1]Corresponding author (e-mail: machtoub@kg8.so-net.ne.jp).

 doi: 10.1139/P06-004

1. Introduction

Systematic studies of the electron–ion interactions involving many-electron ions are needed for exact understanding of formation mechanisms of singly and doubly excited states, their electronic structures, of related complex decay mechanisms by which they relax and of the emitted photon (X-ray) spectra. Plasma diagnostics also benefits from a comparison of the theoretical models with reliable laboratory data. The introduction of an electron beam ion trap (EBIT) has allowed us unprecedented high-resolution measurements of the cross sections for dielectronic recombination (DR), electron-impact ionization and excitation (EIE) of such highly charged ions and made possible a comparison with modern theoretical calculations. As germanium is a useful element for plasma diagnostics, for example, in heated reverse-shear plasmas [1], precision information on its atomic structures, the transition rates of the atomic structures, and line intensity ratios is critically important.

In this work, we calculate the relevant cross sections and extract quantitative information about the electronic structures of highly charged B- to He-like (Ge^{27+}–Ge^{30+}) ions through theoretical investigations of recombination and excitation processes. The numerical and analytical results obtained are related to the electronic charge state distributions, resonance and collision strengths, X-ray wavelengths, decay probabilities, and cross sections. These detailed analyses are used in simulating X-ray emission spectra from trapped highly charged Ge ions interacting with an electron beam, which are then compared with available X-ray measurements from the Heidelberg EBIT. We particularly examine the roles of dielectronic satellites in complex K X-ray spectra, and point out their potentially important applications to the diagnostics of EBIT plasmas.

2. Theoretical analysis

From the theoretical point of view, studies of the recombination and excitation mechanisms for highly charged ions (HCIs) with several inner-shell vacancies and the related cross sections are essential for understanding the spectroscopic characteristics of related transitions and for quantitative explanation of the experimental data. In highly charged ions (X^{q+}), rich radiation spectra of closely spaced X-ray lines originate from the radiative decay of autoionizing states that lie above the ionization limit. These states are created by either the capture of a free electron into ions via dielectronic recombination (DR), forming the doubly excited states

$$X^{q+} + \mathrm{e}(\epsilon) \rightarrow \left[X^{(q-1)+}\right]^{**} \tag{1}$$

or by direct electron-impact excitation (EIE) of one of the inner-shell electrons

$$X^{q+} + \mathrm{e}(\epsilon) \rightarrow \left[X^{q+}\right]^{*} + \mathrm{e}(\epsilon') \tag{2}$$

where $\epsilon' = \epsilon - \Delta\epsilon_{ij} \geq 0$, ϵ being the incident electron kinetic energy and $\Delta\epsilon_{ij}$ the excitation energy from the initial state i to the final state j. When these doubly excited states formed in DR (see (1)) are stabilized radiatively, then the emitted photon (X-ray) is called the dielectronic satellite line.

The DR process of a He-like $Ge^{30+}(1s^2)$ ion takes place when it captures a free electron, meanwhile one of its $1s$-shell electrons is resonantly excited into a higher state, producing a series of the autoionizing resonance states of Ge^{29+} ion, namely, $1snln'l'$ ($n \leq n'$) states. The subsequent radiative transition $1s^2nl$–$1snln'l'$ through the outer (n') or inner (n) shell electron decay produces a photon that forms a series of the dielectronic satellites

$$\mathrm{Ge}^{29+}(1snln'l') \rightarrow \mathrm{Ge}^{29+}(1s^2nl) + h\nu \tag{3}$$

$$\rightarrow \mathrm{Ge}^{29+}(1s^2n'l') + h\nu' \tag{4}$$

In the present work, DR atomic structure calculations are carried out by using the relativistic multi-configuration Hartee–Fock (RMCHF) method [2]. The total resonance strength ($S = \sum S_{ijk}$) is given

Fig. 1. Theoretical DR spectrum convoluted with Gaussian energy distribution of FWHM 33 eV for He-like germanium ions (Ge^{30+}). Resonant transitions reflect different distributions of resonance strengths for KLn ($n = 2$–10), relevant to the outer (dotted line) and inner (continuous line) electron decays.

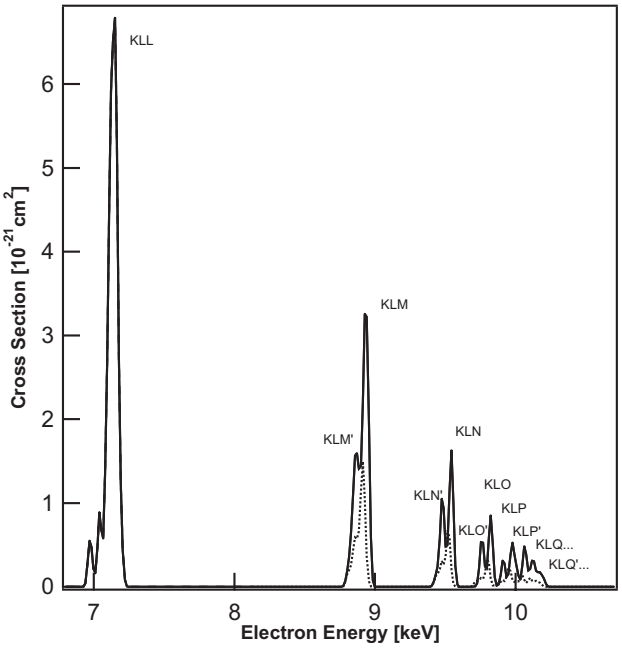

as the sum of the contributions of all individual partial strength from the initial state i through the intermediate doubly excited state j to the final state k

$$S_{ijk} = \int_0^\infty \sigma_{ijk}^{\mathrm{DR}}(E)\,\mathrm{d}E = \frac{\pi^2\hbar^3}{2m_\mathrm{e}E_\mathrm{e}} F_{ijk} \tag{5}$$

where $\hbar$ is the Planck constant, m_e the electron rest mass, E_e the DR resonance energy, $\sigma_{ijl}^{\mathrm{DR}}$ the DR cross section, and F_{ijk} the satellite intensity factor defined in terms of the Auger (A^a) and radiative (A^r) transition rates and the statistical weights of the initial and final states, g_i and g_j, respectively

$$F_{ijk} = \frac{g_j}{g_i} \frac{A_{ji}^\mathrm{a} A_{jk}^\mathrm{r}}{(\Sigma_{i'} A_{ji'}^\mathrm{a} + \Sigma_{k'} A_{jk'}^\mathrm{r})} \tag{6}$$

For comparison with observed K X-ray emission spectra from EBIT the theoretical simulated DR spectrum is constructed using the calculated cross sections for ion with the charge q (σ_q) convoluted with the energy spread of the electron beam as follows:

$$\sigma_{\mathrm{conv}}^{\mathrm{DR}}(E_\mathrm{e}) = \sum_q \frac{1}{\Delta\sqrt{\pi}} \int \exp\left(-\frac{(E_\mathrm{e}-E)^2}{\Delta^2}\right)\sigma_q^{\mathrm{DR}}(E)\,\mathrm{d}E \tag{7}$$

where $\Delta = \omega/(2\sqrt{\ln 2})$, w being the observed FWHM (eV) of the electron beam energy. Here, the DR process is treated as a well-isolated resonant process that occurs independently of the radiative recombination process.

An overview of the theoretical-simulated DR spectra with the detailed structure of the intensity distributions of KLn DR resonances into He-like Ge^{30+} ions due to the decay of the inner (continuous line) or outer (dotted line) electron is shown in Fig. 1. All possible intermediate resonance states $|2lnl'\rangle$

Fig. 2. Schematic energy level diagram illustrating some doubly and singly excited states in Li-like (Ge^{29+}) ions after DR into He-like (Ge^{30+}) ions. The calculated relative percentage decay probabilities associated with resonant transitions, $1s2l2l' \rightarrow 1s^2 2l$, are also shown.

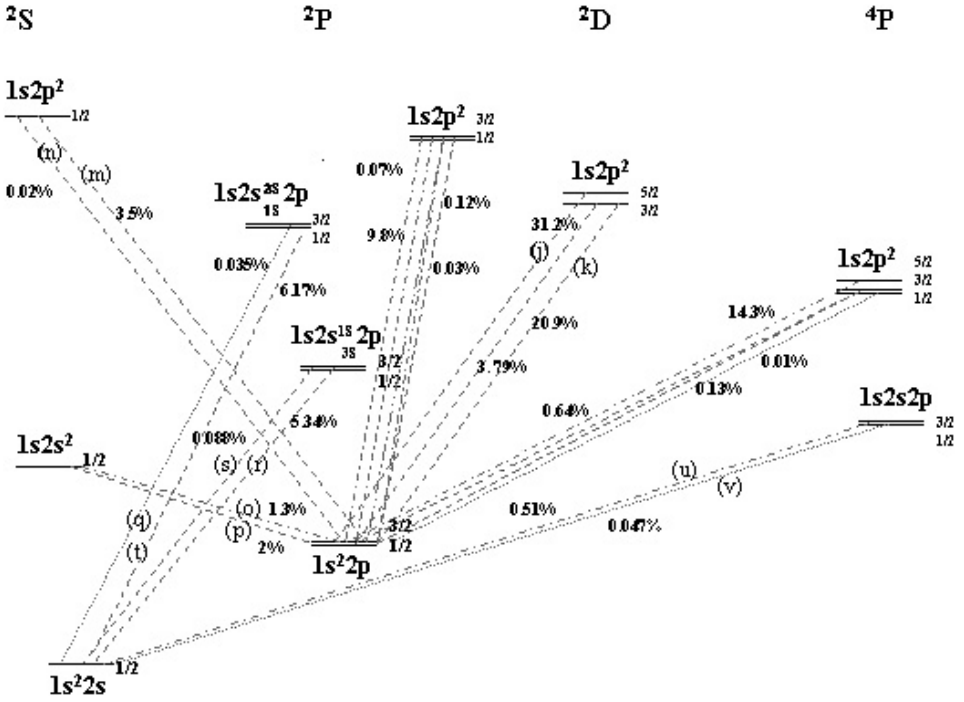

with $n = 2$–10 are included in the calculations of the total resonance strengths. It is clearly shown in Fig. 1 that electrons with energies between 6.9 and 7.2 keV dielectronically recombine with the He-like Ge^{30+} ion, forming Li-like KLL autoionizing $1s2l2l'$ configurations. Among 22 dipole-allowed transitions shown in Fig. 2, the strongest KLL DR transitions that make sizable contributions to the total DR cross sections originate mainly from Li-like doubly excited states $1s2s^2$(3%), $1s2s2p$(12%), and $1s2p^2$(85%) which radiatively decay to either the ground state $1s^2 2s$ or the singly excited states $1s^2 2p$. The predicted relative percentage decay probabilities associated with transitions such as $1s2l2l' \rightarrow 1s^2 2l$ or $1s^2 2l'$ transitions are shown in Fig. 2. The probabilities for the decay to the singly excited states $1s^2 2s$ and $1s^2 2p(\,^2P_{1/2}$ and $\,^2P_{3/2})$ from the doubly excited DR states are obtained by summing the contribution of individual resonance into each singly excited state. The present calculations shown in Fig. 2 indicate that, after the first decay of the doubly excited state formed in DR, the singly excited $1s^2 2s$, $1s^2 2p(\,^2P_{1/2})$, and $1s^2 2p(\,^2P_{3/2})$ states of Li-like ions are occupied with the probabilities of 12%, 23%, and 65%, respectively.

It is established that, in the KLL resonance states, radiative stabilization takes place in most cases via the so-called one- electron-one-photon (OEOP) process. However, some resonance states formed are forbidden to decay directly into the ground state through OEOP process and lead to other transitions such as the two-electron-one-photon (TEOP) decay process. Such simultaneous two-electron transitions accompanying a single-photon emission are labeled in Fig. 2 as "o" and "p" ($1s2s^2 \rightarrow 1s^2 2p(^2P_{1/2,3/2})$. Such TEOP transitions in DR of He-like Ar and Ge-ion spectra have been observed, though weak ($\sim$3%), in recent EBIT measurements [3–5].

Indeed the simultaneous multielectron transitions are of interest both for theoretical and experimental studies, since the observed spectra can be identified more reliably if the characteristics most sensitive

Fig. 3. Theoretical spectra convoluted with the electron beam profile showing branches of KLM and KLN DR for Ge^{30+} ions: Kα (due to the inner decay), Kβ and Kγ (due to the outer decay).

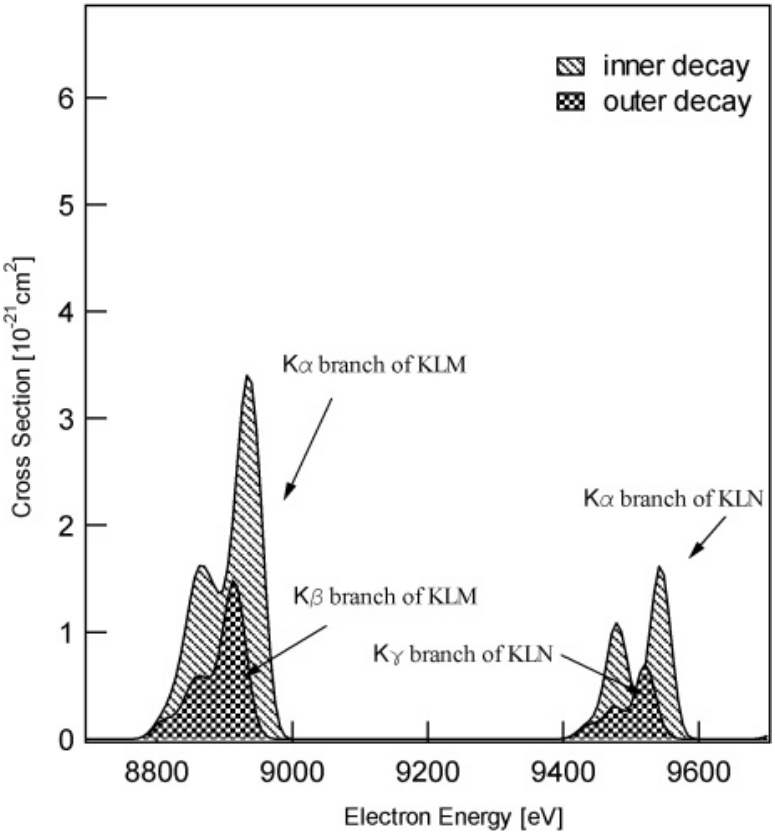

to changes in the electron configurations can be revealed. But so far, the TEOP phenomena have been studied only in processes involving double inner-shell (K) vacancies [6, 7].

The KLM DR resonances occur at higher electron energies (about 8.9 keV for He-like Ge^{30+} ions). In the KLM resonance, one free electron is captured into the M-shell and one of the core (K-shell) electrons in the ion is simultaneously excited to the L-shell, forming an intermediate doubly excited $1s2l3l'$ state. A composition of the X-ray spectrum from the DR KLM ($n = 3$) satellite lines due to the so-called outer ($K\beta$-branch) and inner (Kα-branch) shell electron decays, as shown in Fig. 3, provides information on the electronic structures of ions.

The DR resonances into $n = 4, 5$ are found to occur at the electron energies of about 9.5 and 9.7 keV, respectively. The $1s2l4l'$ (KLN) group of resonances have sufficiently large resonance strengths that contribute significantly to the Kα and Kγ emission as shown in Fig. 3. The $K\beta$ contribution to KLN is almost negligible due to weak cascade ($n = 4 \rightarrow 3$) transitions, where only about 0.05% of the KLN transitions makes a noticeable contribution. The cascades considerably affect the satellite intensity of the $n = 2$ dielectronic satellites that have low Auger decay rates A^a [8, 9].

The KLP DR resonances into $n = 6$ occur at the electron energy of about 9.9 keV, which is almost overlapped at the direct excitation threshold at 10.3 keV.

At somewhat higher energies, an electron recombines with other lower charge ion (Ge^{29+}, Ge^{28+}, Ge^{27+}, …) through DR resonances. For such a target ion a free electron is captured by the ion, producing the resonant states $|1s2s2ln'l'\rangle$, $|1s2s^22pn'l'\rangle$, and $|1s2s^22p^2n'l'\rangle$,…, respectively. The photons That

Fig. 4. Kα spectra from KLL, KLM, KLN, …DR of Li-, Be-, and B-like (Ge^{27+}, Ge^{28+}, Ge^{29+}) ions convoluted with FWHM of 35.3 eV.

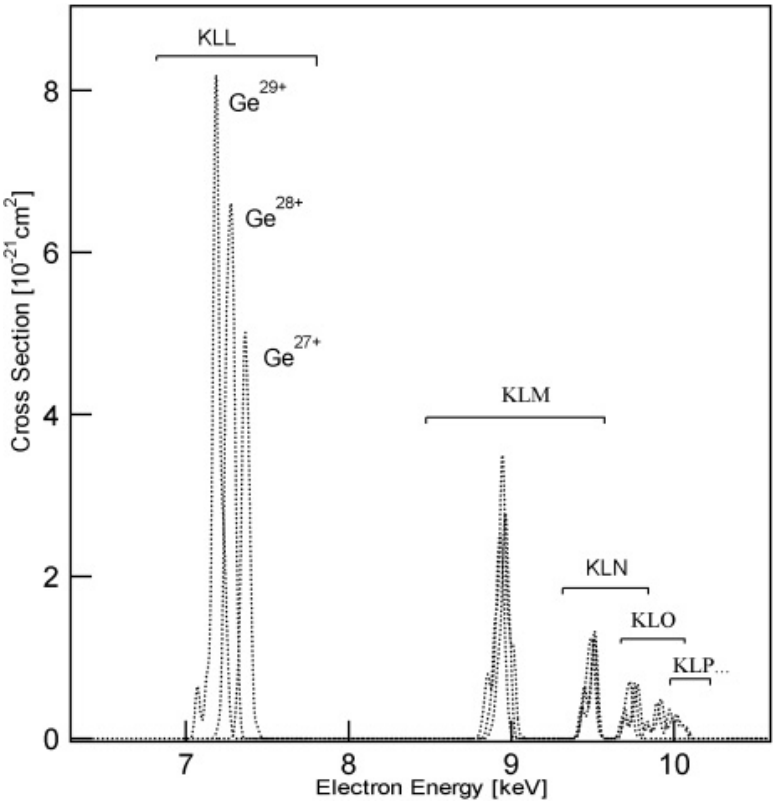

form the DR satellites of these ions are emitted in the subsequent stabilizing radiative transitions

$$\begin{aligned} \mathrm{Ge}^{28+}(1s2s2ln'l') &\rightarrow \mathrm{Ge}^{28+}(1s^2 2s2l) + h\nu, \\ &\rightarrow \mathrm{Ge}^{28+}(1s^2 2sn'l') + h\nu' \end{aligned} \tag{8}$$

and

$$\begin{aligned} \mathrm{Ge}^{27+}(1s2s^2 2pn'l') &\rightarrow \mathrm{Ge}^{27+}(1s^2 2s^2 2p) + h\nu, \\ &\rightarrow \mathrm{Ge}^{27+}(1s^2 2s^2 n'l') + h\nu' \end{aligned} \tag{9}$$

and also

$$\begin{aligned} \mathrm{Ge}^{26+}(1s2s^2 2p^2 n'l') &\rightarrow \mathrm{Ge}^{26+}(1s^2 2s^2 2p^2) + h\nu, \\ &\rightarrow \mathrm{Ge}^{26+}(1s^2 2s^2 2pn'l') + h\nu' \end{aligned} \tag{10}$$

The calculated DR cross sections for lower charge Ge^{27+}–Ge^{29+} ions are shown in Fig. 4.

For HCIs with the ionic charge $q \geq 10$, the radiative decay probability are much larger than the autoionization probability ($A^{\mathrm{r}} >> A^{\mathrm{a}}$) [10]. Since the A^{a} is weakly dependent on the ion charge q whereas the A^{r} increases approximately as $A^{\mathrm{r}} \propto q^4$, the satellites have intensities that increase approximately as q^4. Also their wavelengths are very close to those of the excitation lines. Hence, near the excitation threshold the presence of a large number of spectral lines makes the identification

Table 1. The five parameters obtained by least-squares fitting for some excitation transitions in Ge^{30+}. The numbers enclosed in brackets are powers of 10.

Transition	η_1	η_2	η_3	η_4	ξ
$1s^2(^1S_0) - 1s2s(^3S_1)$	0.00	2.579[−7]	1.831[−5]	1.001[−3]	0.103[+1]
$1s^2(^1S_0) - 1s2p(^1P_1)$	8.556[−3]	−1.036[−2]	2.050[−2]	−8.717[−3]	2.287[−2]
$1s^2(^1S_0) - 1s2p(^3P_0)$	0.00	1.162[−6]	−2.017[−5]	3.494[−4]	4.240[−1]
$1s^2(^1S_0) - 1s2p(^3P_1)$	8.162[−4]	−1.110[−4]	3.523[−4]	−4.136[−5]	−7.206[−1]
$1s^2(^1S_0) - 1s2p(^3P_2)$	0.00	5.523[−6]	−9.571[−5]	1.620[−3]	4.117[−1]

and analysis of the X-ray spectra quite difficult. Though the contribution of the high-n dielectronic satellites calculated theoretically here are important for better X-ray diagnostics, special caution should be exercised if these satellites, near the direct excitation threshold, cannot be resolved experimentally from other DR satellites of the lower charge ions and also from the excitation lines such as Lyman-α doublets. In this work, the atomic structure calculations for EIE cross sections were carried out by using a fully relativistic multiconfiguration code based on the parametric potential method (HULLAC) and in the framework of the distorted-wave approximation (DWA) [11]. The cross section is known to vary smoothly with the electron energy, and it is convenient to fit the dimensionless excitation collision strength to a five-parameter formula for each transition as a function of the electron impact energy in the threshold energy units, $x = \epsilon/\Delta\epsilon_{ij}$, as follows:

$$\Omega_{ij} = \eta_1 ln(x) + \eta_2 + \eta_3/(x+\xi) + \eta_4/(x+\xi)^2 \tag{11}$$

where the $\eta_{1,2,3,4}$ and ξ are parameters obtained by a least-squares fitting for each transition ij [11]. In Table 1 some values are given for the following Ge^{30+} transitions: $1s^2(^1S_0) \rightarrow 1s2s(^3S_1)$, $1s2p(^3P_{0,1,2})$, and $1s2p(^1P_1)$.

Then the electron impact excitation (EIE) cross section is given by

$$\sigma_{ij}^{\mathrm{EIE}} = \frac{\pi a_0^2}{g_i p_i^2}\Omega_{ij} \tag{12}$$

where a_0 is the Bohr radius ($5.291\,772 \times 10^{-9}$ cm), g_i the statistical weight of the initial state, and p_i^2 the squared wave number defined in the relativistic energy-momentum dispersion relation as

$$p_i^2 = \epsilon\left(1 + 0.25\alpha^2\epsilon\right) \tag{13}$$

Here ϵ is the electron kinetic energy in Rydberg units = 13.6057 eV, $\alpha = 7.2974 \times 10^{-3}$ (the fine structure constant $e^2/(\hbar c)$).

The present calculations of EIE cross sections are reported mainly for some principal lines from H-, He-, and Li-like ions: H-like (Ly_{α_2}), He-like (w, y, x, z), Li-like (q, M_2, u, v).

For comparison with the previous EBIT measurements, the KLn (n = 2, 3, 4,…) DR and some of the EIE cross sections of the He-like ion contributing to the Kα X-ray spectrum are shown in Fig. 5. The calculated partial and total excitation (EIE) cross sections for Ge^{30+} ions are shown in the Fig. 5 inset, where the DE cross section is the sum of contributed partial cross sections σ^{EIE} for the following transitions: $1s^2(^1S_0) \rightarrow 1s2s(^3S_1)$, $1s2p(^1P_1)$, and $1s2p(^3P_{0,1,2})$. We summarize in Table 2 the calculated X-ray wavelengths for the following principal lines of He- and H-like ions: (z) $1s^2(^1S_0) - 1s2s(^3S_1)$; ($w$) $1s^2(^1S_0) - 1s2p(^1P_1)$; ($y$) $1s^2(^1S_0) - 1s2p(^3P_1)$; ($x$) $1s^2(^1S_0) - 1s2p(^3P_2)$; ($Ly_{\alpha_2}$) $1s(^2S_{1/2}) - 2p(^2P_{1/2})$.

Fig. 5. Simulated K-shell emission spectra due to DR and EIE for He-like Ge^{30+} ions. The inset shows partial and total EIE cross sections σ^{EIE} for $1s^2 \rightarrow 1s2l$. The direct excitation is the sum of partial EIE contributions for the following excitation transitions: $1s^2(^1S_0) \rightarrow 1s2s(^3S_1)$, $1s2p(^1P_1)$, and $1s2p(^3P_{0,1,2})$. The excitation lines are labeled as z, w, τ, y, and x, respectively.

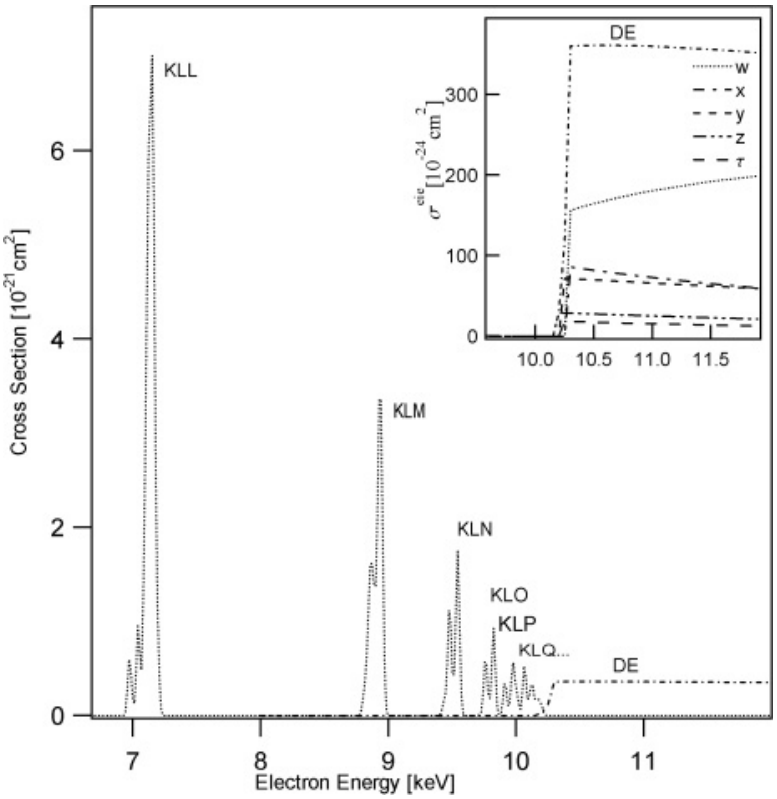

As realized in Table 2, the calculated values of the wavelengths obtained in the present work are found to be in good agreement with available data from Livermore EBIT [12], and results from other theoretical methods [13–15]. Some of Kα lines such as the j-line ($1s2p^2(\,^2D_{5/2}) - 1s^22p(\,^2P_{3/2})$) and the k-line ($1s2p^2(\,^2D_{3/2}) - 1s^22p(\,^2P_{1/2})$) are produced only through DR. The other line of interest is the dipole-forbidden M_2-line ($1s^22s(\,^2S_{1/2}) - 1s2s2p(\,^4P_{5/2})$), which upper state is excited only by the direct EIE from the ground state Li-like ions [16]. Also of particular interest to diagnostics in EBIT- and Tokamak-plasmas are the relative intensity ratios, q(Li-like)/w(He-like), w(He-like)/Ly_α(H-like), Kα_1/Kα_2 and K$\beta_1/K\beta_2$ [17].

Our theoretical predictions for the cross sections producing the population of the upper levels of the Li-like Ge^{29+} (Ge XXX) innershell satellites through the EIE are shown in Fig. 6. Here, special attention has been given to the Li-like resonance line q, $1s^22s(^2S_{1/2})$–$1s2s2p(^2P_{3/2})$, and the magnetic quadrupole-line M_2. Unlike other inner-shell satellites (q, r, s, t, u, v), the dipole-forbidden M_2 transition decreases rapidly as a function of the electron energy. The M_2 transition line has been found to be negatively polarized in high-resolution K X-ray measurements in EBIT [16]. Indeed, this observation has motivated much interest in the predicted electron temperature through the intensity ratio of the M_2 transition line to Li-like resonance line q. The labeled notations (u, v, r, s, t) in Fig. 6 indicate the following transitions: (u) $1s^22s(^2S_{1/2})$–$1s2s2p(^4P_{3/2})$; (v) $1s^22s(^2S_{1/2})$–$1s2s2p(^4P_{1/2})$; (r) $1s^22s(^2S_{1/2})$–$1s2s2p(^2P_{1/2})$; (s) $1s^22s(^2S_{1/2})$–$1s2s2p(^2P_{3/2})$; (t) $1s^22s(^2S_{1/2})$–$1s2s2p(^2P_{1/2})$.

Table 2. Comparison of wavelengths λ, for various transitions of Ge^{30+} and Ge^{31+} ions, calculated in this work with measured wavelengths from Livermore EBIT and other theoretical results.

Ion (line-key)	λ (Å)	λ^{expt} (Å)	λ (Å)	λ (Å)
$Ge^{30+}(w)$	1.20608[a]	1.20599(±21 ppm)	1.20614[b]	1.20606[c]
$Ge^{30+}(x)$	1.20864[a]	1.20848(±36 ppm)	1.20859[b]	1.20857[c]
$Ge^{30+}(y)$	1.21310[a]	1.21294(±34 ppm)	1.21302[b]	1.21307[c]
$Ge^{30+}(z)$	1.21793[a]	1.21776(±51 ppm)	1.21790[b]	1.21788[c]
$Ge^{31+}(Ly_{\alpha_2})$	1.17242[a]	—	1.17245[d]	—

[a] This work using HULLAC.
[expt] The Livermore EBIT [12].
[b] Theoretical work Vainshtein and Safronova [13].
[c] Theoretical work Drake [14].
[d] Theoretical work Johnson et al. [15].

Fig. 6. Theoretical EIE cross sections for forming the inner shell excited Li-like (Ge XXX) satellite lines (q, r, u, v, s, t) and the magnetic quadrupole-line (M_2). EIE cross sections for the resonance q-line increase while the EIE cross sections for the M_2-line decrease rapidly as a function of the electron energy.

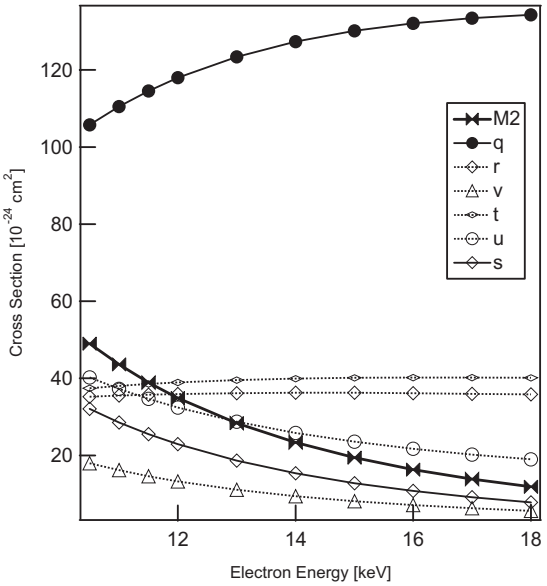

It should be noted that, unlike tokamak plasmas, the line emission from EBIT is strongly anisotropic and polarized as the X-rays emitted by the ions in the trap are produced in collisions with a strongly directional electron beam. The intensity ratio is proportional to the ratio of EIE cross sections (i.e., I_{q_-}(Li-like)/I_w(He-like)$\sim\ \sigma^{ex}_{q_-}/\sigma^{ex}_w$) with the polarization corrections [17], where the notation "q_-" indicates the resonance line q . The intensity ratio is given by

$$\frac{I_{q_-}}{I_w} = \frac{n_{\mathrm{Li}}}{n_{\mathrm{He}}}\frac{\sigma^{\mathrm{ex}}_{q_-}}{\sigma^{\mathrm{ex}}_w}\beta\bar{P} \tag{14}$$

where n_{Li} and n_{He} are the number densities of Li-like and He-like ions, respectively. β is the branching

Fig. 7. (*a*) Predicted EIE cross-section ratio of q-line (Li-like ion) to w-line (He-like), σ_q/σ_w, and (*b*) Li-like EIE cross-section ratios (σ_{M2}/σ_q, σ_u/σ_q, and σ_v/σ_q) as a function of the electron energy.

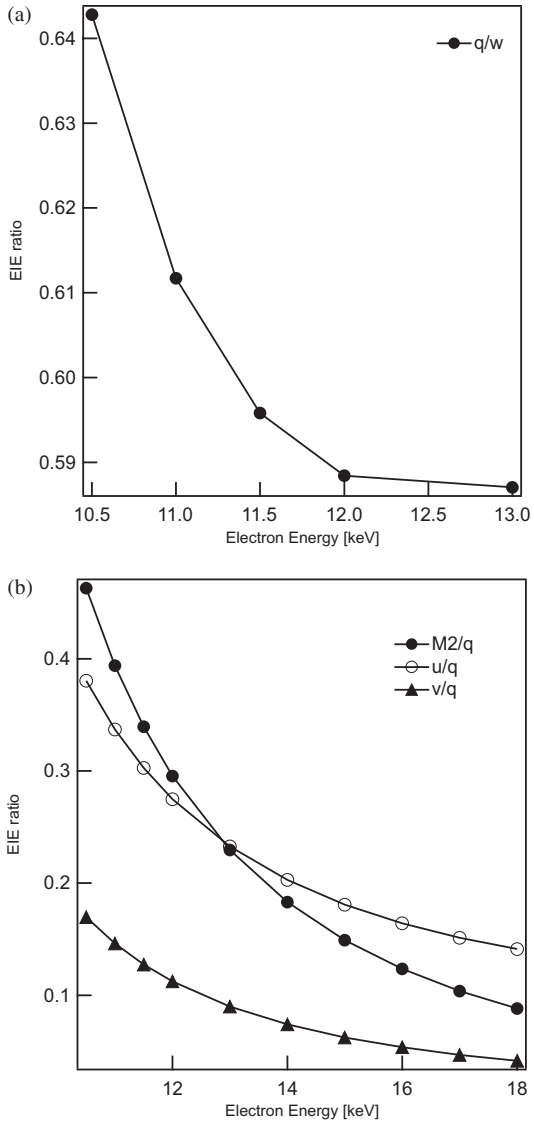

ratio of transitions for the I_{q_-} [18] and $\bar{P}$ is the correction polarization factor given as follows:

$$\bar{P} = \frac{(1+\chi_{q_-}) + R(1-\chi_{q_-})}{(1+\chi_w) + R(1-\chi_w)} \frac{3-\chi_w}{3-\chi_{q_-}} \tag{15}$$

where χ_{q_-} and χ_w are the corresponding polarization degrees of the transitions q and w, and R is the crystal reflectivity parameter. The theoretically predicted EIE cross-section ratio of $q(Ge^{29+})$ to $w(Ge^{30+})$, σ_{q_-}/σ_w, as a function of the electron energy is shown in Fig. 7*a*. Also the predicted electron-energy dependence of Li-like EIE cross-section ratios (σ_{M2}/σ_{q_-}, σ_u/σ_{q_-}, and σ_v/σ_{q_-}) is shown in Fig. 7*b*.

Table 3. Comparison of ionization energies $I_{\rm pot}$ in (eV) for ions (Ge^{27+}–Ge^{31+}) calculated in the present work using HULLAC (*a*) with available results from other theoretical methods: (*b*) Boiko et al. [19], (*c*) Carlson et al. [20], and (*d*) Biemont et al. [21].

$I_{pot}(Ge^{31+})$	$I_{\rm pot}(Ge^{30+})$	$I_{\rm pot}(Ge^{29+})$	$I_{\rm pot}(Ge^{28+})$	$I_{\rm pot}(Ge^{27+})$
$14119.00^{(a)}$	$13556.00^{(a)}$	$3194.00^{(a)}$	$3066.00^{(a)}$	$2885.00^{(a)}$
$14119.50^{(b)}$	$13557.20^{(b)}$	$3194.179^{(d)}$	$3066.304^{(d)}$	$2885.023^{(d)}$
$13670.00^{(c)}$	$13090.00^{(c)}$	$3125.00^{(c)}$	$2995.00^{(c)}$	$2787.00^{(c)}$

3. Comparison with measurements

In earlier experimental investigations [4, 5], the analysis was focused on the KLL DR resonances of He-like ions. In the present work, we have further extended the detailed descriptions to all the ions with different charges (He-, Li-, Be-, and B- like ions) taking into account their abundances relevant to the EBIT experiments. The present analysis includes the contribution of all possible high-lying states (through the inner and outer decays) of KL*n* DR resonances, along with the contributions from EIE processes near the excitation threshold. The theoretical simulated spectra from the trapped highly charged germanium ions are then compared and fitted to the observed K X-ray emission spectra over a wide range of electron energy.

At Heidelberg EBIT experiments, X-ray measurements from Ge ions in various charge states were carried out while the electron beam energy was ramped over a wide range (6.7–11.1 keV). The electron beam was kept at around 100 mA, and the magnetic field in the trap region was set to 8 T. The low-charge-state ions injected from a laser ion source were successively ionized through collisions with a dense electron beam. The X-ray signals were accumulated with a multiparameter data acquisition system in which both the electron and the X-ray energies were recorded simultaneously. The interacting electron beam energy $E_{\rm ebeam}$ was determined from the X-ray energy $E({\rm RR})_{\rm Xray}$ due to radiative recombination (RR) and the known ionization potential $I_{\rm pot}$ of the ion formed after recombination using the following equation:

$$E_{\rm ebeam} = E({\rm RR})_{\rm Xray} - I_{\rm pot} \tag{16}$$

The ionization potentials for H-, He-, Li-, Be-, and B-like (Ge^{27+}–Ge^{31+}) ions calculated with HULLAC are listed in Table 3. The calculated values in the present work are in close agreement with available results from other theoretical methods [19–21].

The theoretical simulated DR spectra $I^{\rm DR}$ are expressed by the sum of the cross sections (see (7)) of different charge states as follows:

$$I^{\rm DR} = \rho \sum_q a_q \sigma_q^{\rm DR}(q, E) \tag{17}$$

where a_q is a fractional abundance of the trapped highly charged Ge ions with the charge q and is given as $a_q = n_q/n_{\rm T}$, where n_q is the number density of ions with the charge state q, and $n_{\rm T}$ the total number density of the ionic species in the trap ($n_{\rm T} = \sum_q n_q$).

The normalization factor ρ at a particular electron energy E is

$$\rho = I^{{\rm RR}_{n=2}} \left(\frac{3}{3 - P^{\rm RR}} \sum_q a_q \sigma^{{\rm RR}_{n=2}}(q, E) \right)^{-1} \tag{18}$$

where $I^{{\rm RR}_{n=2}}$ is the observed intensity of RR photons at $n = 2$, $\sigma^{{\rm RR}_{n=2}}$ the theoretical cross section for radiative recombination onto the $n = 2$ shell ($\rm RR_{n=2}$), $P^{\rm RR}$ the average RR polarization degree. Then

Fig. 8. Theoretical simulated spectra (dotted line), convoluted with the electron beam energy profile, including the partial DR contributions of the mixed-charge Ge^{27+}–Ge^{30+} ions. The total simulated spectrum is compared with the observed Kα X-ray spectra (continuous line) obtained at Heidelberg EBIT [7].

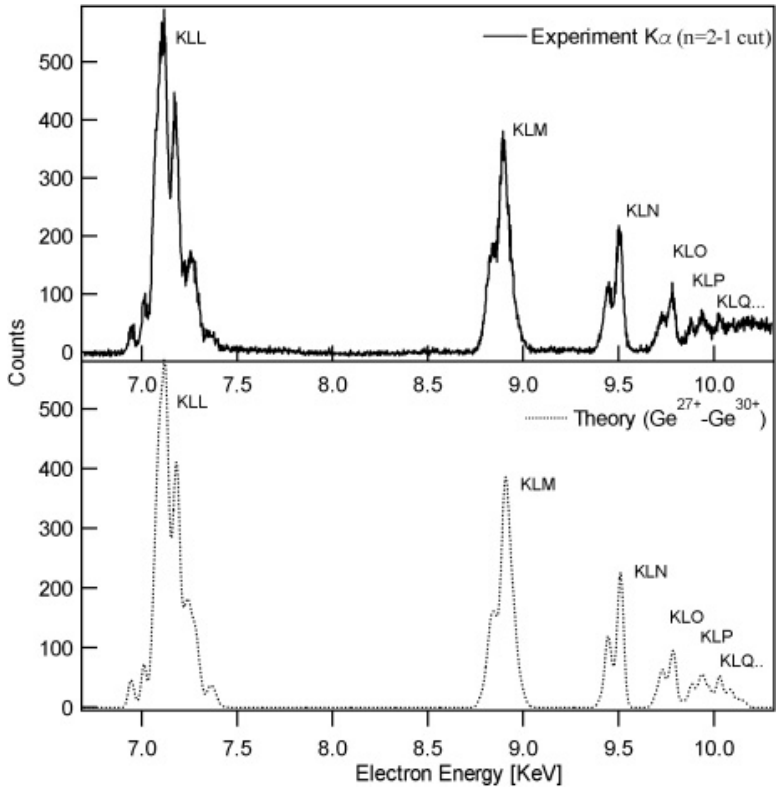

the average ion density $\bar{n}_{\rm ion}$ can be estimated from $\bar{n}_{\rm ion} = \rho/(\frac{J_{\rm e}}{e}\frac{\Delta\Omega}{4\pi})$, where $\Delta\Omega$ is the solid angle of the X-ray detector and $J_{\rm e}$ the electron current density [22].

The angular distributions of the emitted DR X-rays can be described with the cross section $\sigma_q^{\rm DR}(90°) \equiv \sum_j \Theta_j(90°)\sigma^{\rm DR}$, where $\sigma^{\rm DR}$ is the total space-integrated DR cross section and $\Theta_j(90°) = 3/(3-\chi_j)$, χ_j being the polarization degree for radiative decay from the state "j". In the isolated resonances, the linear polarization degrees χ for He-, Li-, and Be-like ions are calculated assuming that the doubly excited states are populated through the electron recombination only into target ions in the ground state. We have calculated the $\Theta(90°)$ values for all possible transitions and weighted the results according to the statistical populations. For the degree of the linear polarization associated with $\Delta J = (J_j - J_k) = 1$ stabilizing transitions, the angular correction factors are taken to be $\chi = 0.5$–0.6 ($\Theta(90°) = 1.2$–1.25) for He- and Be-like ions and $\chi = 0.43$–0.6 ($\Theta(90°) = 1.16$–1.5) for Li-like ions. The remaining resonances are assumed to produce X-ray lines that have the negative polarizations (i.e., $\chi = -0.428$, -0.60, -0.75, …, -1.0) or are unpolarized ($\chi = 0$) [23].

To compare these predictions with those of the measured X-ray spectrum, the calculated DR resonance strengths were convoluted with the Gaussian profile of the electron energy distributions, where ω(FWHM) = 33 eV corresponding to $\Delta^2 = 390$ (see 7).

The simulated spectra from the mixed charge ions (Ge^{27+}–Ge^{30+}) are then fitted to the observed spectra as shown for the Kα-cut ($n = 2 \rightarrow 1$ decay) in Fig. 8. The normalization factor ρ (18) is determined in the course of fitting procedure. Using the least-squares method [24], the ion fractional

Table 4. Total resonance strengths S for different DR states of He-like Ge ions in units of 10^{-20}cm^2 eV.

Resonance	KLL	KLM	KLN	KLO
$S(Ge^{30+})$	63.65	34.95	14.52	6.87

Fig. 9. A comparison of theoretical convoluted DR spectra for He-like Ge^{30+} ions with experimental spectra along RR($n = 2$) cut. Some discrepancy at the high-energy shoulder of the KLM resonance is due to omission of the DR contribution from the lower charged ions.

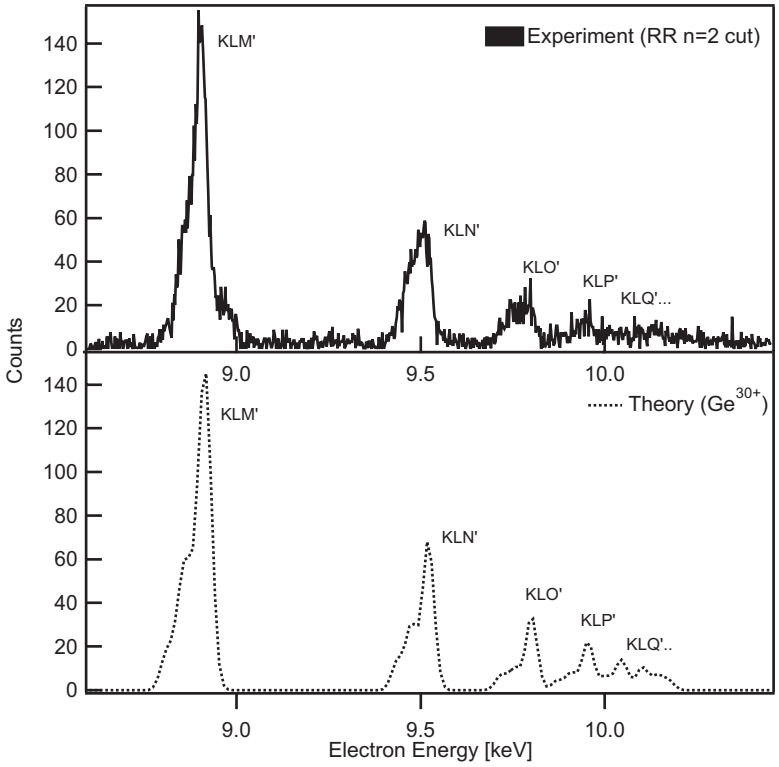

abundance a_q was obtained after several iterations where the sum is normalized to unity ($\sum_q a_q$=1). It should be noted that discrepancies at higher energies beyond the excitation threshold (10.3 keV) are mainly due to the EIE contribution shown in Figs. 5 and 6. The calculated EIE cross sections folded into the experimental resolution and then summed can be well-fitted to the observed data over the energy range (10.3–11.1 keV), adding the EIE sum to $\Delta n = 1$ transitions of DR cross sections (obtained by the n^{-3} near the excitation threshold) as well as those of $\Delta n = 2$ transitions of DR overlapping the direct excitation continua. In the present work, the possible contributions arising from $\Delta n = 2$ DR KMn ($n \geq 3$) resonances and the resonant excitation due to Auger decay to a bound state different from the initial state have been neglected. We have found good overall agreement of our theoretical simulated spectra with the observed spectra from ions with mixed charge distributions obtained in EBIT measurements.

The present calculated total resonance strengths of KLn ($n = 2$–5, namely, KLL, KLM, KLN, and KLO) DR for He-like Ge ions are given in Table 4.

The agreement has been found to be quite good in comparison with the measured resonance strengths (S^{EBIT}) in ref. 5, i.e., $S^{\mathrm{EBIT}}(\mathrm{KLL}) = 63.7 \pm 7.5 \times (10^{-20}\ \mathrm{cm^2 eV})$, and with the values ($S^{\mathrm{e}}$) obtained upon an empirical formula previously proposed [25]. The values of S^{e} obtained in units of (10^{-20} cm^{2}eV) for KLL, KLM, KLN, and KLO are 65.37, 35.32, 14.70, and 7.35, respectively.

Furthermore, the convoluted simulated DR spectra of He-like (Ge^{30+}) ions for the outer-shell electron decay is compared with the observed spectra along the RR($n = 2$) cut shown in Fig. 9. Overall agreement between them is observed except for some discrepancy at the high-energy shoulder of the KLM resonances as the contribution of DR from the lower charge state (Li-, Be-, B-like) ions is not included in the simulated spectra.

In conclusion, we have presented our detailed theoretical analysis on the dielectronic (and radiative) recombination and excitation transitions for highly charged germanium ions. This has allowed us to extract quantitative information about the ionic structures and electron–ion collision dynamics. Our calculations of these cross sections have been used to explain the details of the resonant structures in the observed K X-ray spectra and shown good overall agreement with high-resolution X-ray measurements available from EBIT over a wide range of the electron energy. Some useful diagnostic aspects relevant to EBIT plasmas are also presented. The theoretically predicted EIE–cross section ratios for Ge ions have been found to provide useful information on the electron temperature measurements of plasmas.

Acknowledgements

The author acknowledges funding support from the Ministry of Education, Science, and Culture in Japan and also the collaboration with Japan Atomic Energy Research Institute as part of the present work was performed using HULLAC.

References

1. M. May, K. Fournier, M. Mattioli, D. Pacella, M. Finkenthal, L. Gabellieri, G. Mazzitelli, W.H. Goldstein, and H.W. Moos. 27th EPS Conference on Contr. Fusion and Plasma Phys. Budapest, 12–16 June 2000 ECA. Vol. **24B**, 284 (2000).
2. R.D. Cowan. Theory of atomic structure and spectra. University of California Press, Berkley, Calif. 1981.
3. Y. Zou, J.R. Crespo López-Urrutia and J. Ullrich. Phys. Rev. A, **67**, 042703 (2003).
4. V. Mironov, M. Trinczek, A. Werdich, A.J. González Martínez, P. Guo, X. Zhang, J. Braun, J.R. Crespo López-Urrutia, and J. Ullrich. Nucl. Instrum. Method B, **205**, 183 (2003).
5. X. Zhang, J.R. Crespo López-Urrutia, P. Guo, V. Mironov, X. Shi, A.J. González Martínez, H. Tawara, and J. Ullrich. J. Phys. B: At. Mol. Opt. Phys. **37**, 2277 (2004).
6. R. Schuch, G. Gaukler, and H. Schmidt-Böcking. Z. Phys. A, **90**, 19 (1979).
7. J. Volpp, R. Schuch, G. Helte, and H. Schmidt-Böcking. J. Phys. B: At. Mol. Opt. Phys. **12**, L325 (1979).
8. R. Ali, C. Bhalla, C.L. Cocke, M. Schulz, and M. Stockli. Phys. Rev. A, **44**, 223 (1991).
9. O. Marchuk, G. Bertschinger, H.-J. Kunze, N.R. Badnell, and S. Fritzsche. J. Phys. B: At. Mol. Opt. Phys. **37**, 1951 (2004).
10. H. Beyes and V. Shevelko. Introduction to the physics of highly changed ions. IOP Publishing, Bristol, U.K. 2003.
11. A. Bar-Shalom, M. Klapisch, and J. Oreg. Phys. Rev. A, **38**, 1773 (1988).
12. S. MacLaren, P. Beiersdorfer, D.A. Vogel, D. Knapp, R.E. Marrs, K. Wong, and R. Zasadzinski. Phys. Rev. A, **45**, 329 (1992).
13. L.A. Vainshtein and U.I. Safronova. Phys. Scr. **31**, 519 (1985).
14. G.W. Drake. Can. J. Phys. **66**, 586 (1988).
15. W.R. Johnson and G. Soff. At. Data Nucl. Data Tables, **33**, 405 (1985).
16. P. Beiersdorfer, M. Bitter, D. Hey, and K.J. Reed. Phys. Rev. A, **66**, 032504 (2002).
17. J. Peacock, R. Barnsley, M.G. O'Mullane, M.R. Tarbutt, D. Crosby, J.D. Silver, and J.A. Rainnie. Rev. Sci. Instrum. **72**, 1250 (2001).
18. M.S. Chen. At. Data Nucl. Data Tables, **34**, 301 (1986).

19. V.A. Boiko, V.G. Palćhikov, I.Yu. Skobelev, and A.Ya. Faenov. Atomic spectroscopical constants. Moscow, Standarts, (1988).
20. T.A. Carlson, C.W. Nestor, N. Wasserman, J.D. McDowell. At. Data Nucl. Data Tables, **2**, 63 (1970).
21. E. Biemont, Y. Fremat, P. Quinet. At. Data Nucl. Data Tables, **71**, 117 (1999).
22. R. Radtke, C. Biedermann, T. Fuchs, and G. Fussmann. Phys. Rev. E, **61**, 1966 (2000).
23. G. Machtoub. Can. J. Phys. **81**, 1177 (2003).
24. W.H. Press, S.A. Teukolsky, W.T. Vetterling, and B.P. Flannery. Numerical recipes in Fortran 77. Cambridge University Press, N.Y. **675**, (1989).
25. H. Watanabe, F.J. Currell, H. Kuramoto, Y. Li, S. Ohtani, B. O'Rourke, and X. Tong. J. Phys. B: At. Mol. Opt. Phys. **34**, 5095 (2001).